



HAL
open science

Volumetric Properties of Binary Mixtures of 1,2-Dichloroethane with Ethers from 278.15–333.15 K and at Atmospheric Pressure

Alain Valtz, Esther Neyrolles, Farid Brahim Belaribi, Christophe Coquelet

► **To cite this version:**

Alain Valtz, Esther Neyrolles, Farid Brahim Belaribi, Christophe Coquelet. Volumetric Properties of Binary Mixtures of 1,2-Dichloroethane with Ethers from 278.15–333.15 K and at Atmospheric Pressure. *Journal of Chemical and Engineering Data*, 2022, 67 (3), pp.554-567. 10.1021/acs.jced.1c00810 . hal-03574360

HAL Id: hal-03574360

<https://hal.science/hal-03574360>

Submitted on 15 Feb 2022

HAL is a multi-disciplinary open access archive for the deposit and dissemination of scientific research documents, whether they are published or not. The documents may come from teaching and research institutions in France or abroad, or from public or private research centers.

L'archive ouverte pluridisciplinaire **HAL**, est destinée au dépôt et à la diffusion de documents scientifiques de niveau recherche, publiés ou non, émanant des établissements d'enseignement et de recherche français ou étrangers, des laboratoires publics ou privés.

Volumetric properties of binary mixtures of 1,2-dichloroethane with ethers from 278.15 – 333.15 K and at atmospheric pressure

Alain Valtz^a, Esther Neyrolles^a, Farid Brahim Belaribi^b, Christophe Coquelet^{a,c}

^aMines ParisTech, PSL University, CTP-Centre of Thermodynamics of Processes, 35 Rue Saint Honoré, 77305 Fontainebleau, France

^bThermodynamic and Molecular Modelisation Laboratory, Faculty of Chemistry, University of Sciences and Technology Houari Boumediene (USTHB), B.P. 32 El-Alia, Bab-Ezzouar, Algiers, Algeria

^cUniversité de Toulouse, IMT Mines Albi, UMR CNRS 5302, Centre Rapsodee, Campus Jarlard, 81013 Albi CT Cedex 9, France

email: christophe.coquelet@mines-albi.fr

Abstract

Using a vibrating tube density meter, the densities and speed of sound of 1,2-dichloroethane, methyl tert-butyl ether, diisopropyl ether, and diethyl ether were measured between $T = (278.15 \text{ to } 333.15) \text{ K}$ and at atmospheric pressure. The densities of the three binary mixtures: 1,2-dichloroethane + ethers, were also experimentally determined. The Redlich-Kister data treatment and partial molar volume were applied to the excess molar volume of the mixtures. To conclude, the Prigogine-Flory-Patterson model was used to predict the excess molar volume of the three binary systems and to determine the most significant contribution to the excess molar volume.

Keywords: Excess molar volume, apparent molar volume, partial molar volume, vibrating densitometer

1. Introduction

Thermodynamic properties of a pure compound or multi-compound mixtures are highly required in the context of the chemical and process industry. They are necessary to design, model, and optimize industrial processes, current or new ones. These properties can be experimentally measured or estimated with thermodynamic models or correlations. The 1,2-dichloroethane (DCE), the methyl tert-butyl ether also known as 2-methoxy-2-methylpropane (MTBE), the diisopropyl ether also known as 2-propan-2-yloxypropane (DIPE), and the diethyl ether also known as ethoxyethane (DEE) belongs to two important groups of molecules in chemistry: chloroalkanes and ethers. Both of them are widely used in the chemical industry as a solvent for extraction or chemical reaction, refrigerants, etc., but also in other industries like in the pharmaceutical industry^{1,2}. The volumetric properties like density and speed of sound for pure compound and mixing density and excess molar volume for the mixtures are really important in several units operation of the chemical engineering industry such as distillation columns, liquid-liquid extractors, etc. The excess molar volume gives information on the interaction between the molecules in the mixture. The influence of –O– and –Cl group interaction between the DCE and the ethers is of interest here. These molecular interactions are essential for the development of appropriate thermodynamic models to design industrial processes. In line with experimental and theoretical previous works³⁻⁶ on DCE with ether, this study presents the experimental densities of the three mixtures DCE + MTBE, DCE + DIPE, and DCE + DEE between $T = (278.15 \text{ to } 333.15) \text{ K}$. In this work, we start by a presentation of the theory considered to correlate the experimental data. Then the experimental apparatus is described. To continue, the results are presented and the excess molar volume estimated is compared with the Redlich-Kister correlation⁷. And lastly, the Prigogine-Flory-Patterson (PFP) theory⁸⁻¹¹ is used to determine the main contribution of the interactions between the molecules.

2. Theory section

The excess molar volume v^E of a solution is expressed following Eq. 1:

$$v^E = v - x_1 v_1^0 - x_2 v_2^0 \quad (1)$$

where x_1 , x_2 , v_1^0 and v_2^0 represent respectively the mole fractions and molar volumes of DCE (1) and ether (2). Eq. 1 can be rewritten as:

$$v^E = \left[\frac{x_1 M_1 + x_2 M_2}{\rho} \right] - \frac{x_1 M_1}{\rho_1} - \frac{x_2 M_2}{\rho_2} \quad (2)$$

where M_1 , M_2 , ρ_1 and ρ_2 represent respectively the molar masses and densities of DCE (1) and ether (2) and ρ represent the density of the mixture.

2.1. Redlich-Kister correlation

The Redlich-Kister (RK) correlation⁷ is chosen to correlate excess molar volume of binary systems:

$$v^E = x_1 x_2 \sum_i A_n (x_1 - x_2)^i \quad (3)$$

where A_n is the RK coefficient.

The Redlich-Kister coefficients A_n are adjusted at each temperature studied. The standard deviation σ corresponding to each fit is estimated following Eq 4:

$$\sigma = \sqrt{\sum \frac{(v^E - v_{cal}^E)^2}{N_{exp} - P}} \quad (4)$$

where P is the number of RK coefficients and N_{exp} is the number of experimental data. The maximum number of RK coefficients is chosen to have σ lower than the excess molar volume uncertainty.

2.2. Partial molar volume

The partial molar volume v_i ($\text{cm}^3 \cdot \text{mol}^{-1}$) of each component is calculated following Eq 5:

$$v_i = \left(\frac{dV}{dn_i} \right)_{T,P,n_j} \quad (5)$$

After differentiation of Eq 1 concerning n_i and combining the result to Eq 5. It leads to Eqs 6 and 7 for the partial molar volumes of the different species.

$$v_1 = v^E + v_1^0 - x_2 \left(\frac{dv^E}{dx_2} \right)_{T,P} \quad (6)$$

$$v_2 = v^E + v_2^0 - x_1 \left(\frac{dv^E}{dx_1} \right)_{T,P} \quad (7)$$

The expressions of partial molar volumes, for x_i , are obtained, by using the Redlich-Kister equation, following Eq 8 and 9:

$$v_1 = v_1^0 + x_2^2 \sum A_n (1 - 2x_2)^n + 2x_2^2 (1 - x_2) \sum n A_n (1 - 2x_2)^{n-1} \quad (8)$$

$$v_2 = v_2^0 + (1 - x_2) \sum A_n (1 - 2x_2)^n - 2x_2^2 (1 - x_2) \sum n A_n (1 - 2x_2)^{n-1} \quad (9)$$

At infinite dilution, the partial molar volume is identical to the apparent molar volume $v_{\phi 1}$. The apparent molar volume of DCE in ether $v_{\phi 1}$ is given by Eq. 10:

$$v_{\phi_1} = \frac{v - x_2 v_2^0}{x_1} \quad (10)$$

The combination of Eq. 10 and Eq. 1 leads to Eq. 11 for apparent molar volume v_{ϕ_l} of DCE in ether.

$$v_{\phi_1} = v_1^0 + \frac{v^E}{x_1} \quad (11)$$

2.3 Prigogine-Flory-Patterson theory

The Prigogine-Flory-Patterson (PFP) theory⁸⁻¹¹ is widely applied to predict excess thermodynamics properties such as the excess molar volume, v^E . Originally, the Flory model was used to explain the thermodynamic behavior of non-polar mixtures but the model can be used with polar mixture considering Flory parameter adjusted on experimental data following Hansen's theory¹². In this study, excess properties of the mixtures are linked to the measurable macroscopic properties of the pure constituents.

According to the PFP model, the excess molar volume is the sum of three contributions listed below:

- The interactional contribution v_{int} is proportional to the empirical Flory parameter χ_{12} which can be adjusted from experimental excess molar volumes, following Eq 12:

$$v_{int} = \frac{(\tilde{v}^{1/3} - 1)\tilde{v}^{2/3}}{(4/3)\tilde{v}^{-1/3} - 1} \psi_1 \theta_2 \frac{\chi_{12}}{P_1^*} \quad (12)$$

- The free volume contribution v_{fv} is due to the difference between the thermal expansions of the two components, following Eq 13:

$$v_{fv} = \frac{(\tilde{v}_1 - \tilde{v}_2)^2 [(14/9)\tilde{v}^{1/3} - 1]}{(4/3)\tilde{v}^{-1/3} - 1} \psi_1 \psi_2 \quad (13)$$

- The P^* contribution (internal pressure contribution) v_{P^*} is dependent on both the differences between the reduced volumes and internal pressures of the two molecules, following Eq 14:

$$v_{P^*} = \frac{(\tilde{v}_1 - v)^2 (P_1^* - P_2^*)}{P_1^* \psi_2 + P_2^* \psi_1} * \psi_1 \psi_2 \quad (14)$$

\tilde{v} is the reduced volume ($\tilde{v} = \psi_1 \tilde{v}_1 + \psi_2 \tilde{v}_2$), ψ_i is the molecular contact energy ($\psi_1 = 1 - \psi_2 = \frac{\varphi_1 P_1^*}{\varphi_1 P_1^* + \varphi_2 P_2^*}$). The hardcore volume fraction φ_i is given by $\varphi_1 = 1 - \varphi_2 = \frac{x_1 v_1^*}{x_1 v_1^* + x_2 v_2^*}$.

θ_2 is the molecular surface fraction ($\theta_2 = \frac{\varphi_2}{\varphi_1 (S_1/S_2) + \varphi_2}$) with the ratio S_1/S_2 approximates by $(V_2^*/V_1^*)^{1/3}$ according to Abe and Flory¹⁰.

\tilde{v}_i is the reduced volume defined in Eq 15:

$$\tilde{v}_i = \left[\frac{1 + \left(\frac{4}{3}\right) \alpha_i T}{1 + \alpha_i T} \right]^3 \quad (15)$$

The thermal coefficient expansion α_i is given by $\alpha_i = (1/v_i^0)(\partial v_i^0 / \partial T)_P$. v_i^* and P_i^* are respectively the characteristic volume ($v_i^* = \frac{v_i}{\tilde{v}_i}$) and pressure ($P_i^* = \frac{T \tilde{v}_i^2 \alpha_i}{\kappa_{Ti}}$).

The isothermal compressibility κ_{Ti} is given by $\kappa_{Ti} = -(1/v)(\partial v / \partial T)_T$

The isothermal compressibility κ_{Ti} is also related via Maxwell's relation (Eq. 16) to the isentropic compressibility κ_s .

$$\kappa_{Ti} = \kappa_{Si} + \alpha_i^2 V_i \frac{T}{C_{pi}} \quad (16)$$

where V_i is the molar volume of the compound i and C_{pi} is the liquid heat capacity. The isentropic compressibility κ_{Si} can be estimated using the density ρ_i and the speed of sound u_i of a compound ($u_i = \sqrt{\frac{1}{\kappa_{Si}\rho_i}}$).

Consequently, in the terms of the three contributions to the PFP theory, the excess molar volume is given by Eq. 17:

$$\begin{aligned} \frac{v^E}{x_1 v_1^* + x_2 v_2^*} = v_{int} + v_{fv} + v_{P^*} = & \frac{(\frac{1}{\bar{v}^3} - 1) \bar{v}^{\frac{2}{3}}}{(\frac{4}{3}) \bar{v}^{-\frac{1}{3}} - 1} \psi_1 \theta_2 \frac{\chi_{12}}{P_1^*} + \frac{(\bar{v}_1 - \bar{v}_2)^2 \left[\left(\frac{14}{9} \right)^{\frac{1}{3}} - 1 \right]}{(\frac{4}{3}) \bar{v}^{-\frac{1}{3}} - 1} \psi_1 \psi_2 \\ & + \frac{(\bar{v}_1 - \bar{v}_2)^2 (P_1^* - P_2^*)}{P_1^* \psi_2 + P_2^* \psi_1} \psi_1 \psi_2 \end{aligned} \quad (17)$$

3. Experimental section

3.1. Chemicals

The list of chemical species used is presented in Table 1, with the suppliers and the purities. Chemicals were used without any further purification.

Table 1: Chemical sample

Chemical name	Abbreviation	CAS number	Source	Mole Fraction Purity reported by the supplier	Analysis Method
1,2-dichloroethane	DCE	107-06-2	Acros organics	0.998	GC ^a
2-methoxy-2-methylpropane	MTBE	1634-04-4	Acros organics	0.999	GC ^a
2-propan-2-yloxypropane	DIPE	108-20-3	Merck	0.985	GC ^a
ethoxyethane	DEE	60-29-7	Acros organics	0.990	GC ^a

^aGC: Gas chromatograph

3.2. Apparatus

Density measurements have been made with the DSA5000M Anton Paar digital vibrating tube density meter. The experimental equipment has already been described in the previous studies^{3,13,14}, only a few essentials are given here. The tube mass of the density meter and so the fluid density are dependent of the oscillating period or frequency. The period of vibration τ is related to density ρ_i following Eq. 18, where a and b are constants to be adjusted.

$$\rho_i = a + b \tau^2 \quad (18)$$

The density meter was checked at $T = 293.15$ K with dry air and de-gassed bi-distilled ultra-pure water. The temperature is measured with a platinum resistance thermometer (0.01 K accuracy). When the density meter is at thermal equilibrium, the sample densities are measured. Mixtures were prepared by weighing, with uncertainty in mole fraction estimated to be less than 0.002. All weighing performed in the experimental work was carried out using a Mettler balance, with a precision of \pm

1.10^{-4} g. As recommended by Chirico and al.¹⁵, the purities of each compound x_{is} , presented in Table 1, are taken into account for the estimation of the expanded uncertainties. The maximum uncertainty on measured density is estimated to be: $u(\rho_i) = 1.5 \text{ kg.m}^{-3}$. For the excess molar volumes, the maximum $u(v^E)$ is estimated to be $\pm 0.011 \text{ cm}^3.\text{mol}^{-1}$.

To estimate the uncertainty of the mole fraction $u(x_i)$, the density $u(\rho_i)$ of the compound i , the density of the mixture $u(\rho)$ and the excess molar volume $u(v^E)$, the following Eqs 19 to 22 were used:

$$u(\rho_i) = \xi (1 - x_{si}) \quad (19)$$

$$u(x_i) = x_1 x_2 (1 - x_{s1})(1 - x_{s2}) \sqrt{\frac{1}{(m_1)^2} + \frac{1}{(m_2)^2}} \quad (20)$$

$$u(\rho) = \sqrt{u(\rho_1)^2 + u(\rho_2)^2 + u(x_i)^2} \quad (21)$$

$$u(v^E) = \sqrt{\left[\left(\frac{x_1 M_1 + x_2 M_2}{\rho^2} \right)^2 + \left(\frac{x_1 M_1}{\rho_1^2} \right)^2 + \left(\frac{x_2 M_2}{\rho_2^2} \right)^2 \right] u(\rho)^2 + \left(\frac{M_1 + M_2}{\rho} - \frac{M_1}{\rho_1} - \frac{M_2}{\rho_2} \right)^2 u(x_i)^2} \quad (22)$$

where ξ is the presumed difference in density between the compound and the impurity. We have chose to use $\xi = 0.1$ as recommended by Chirico and al.¹⁵.

This density meter is also used to measure the speed of sound u_i with an uncertainty of 0.5 m.s^{-1} .

The density meter is not equipped with a pressure transducer. In consequence, the value of atmospheric pressure is given by a GE Druck DPI 142, Precision Barometric Indicator with standard uncertainty $u(p) = 0.035 \text{ kPa}$. We have considered as uncertainty on atmospheric pressure the variation of atmospheric pressure during the experiment which was lower than 0.1 kPa .

4. Results

The densities and the speed of sound of the four pure compounds measured by the DSA 5000M Anton Paar density meter, between $T = (278.15 \text{ to } 333.15) \text{ K}$ and at atmospheric pressure, are presented in Table 2. The experimental data concerning the densities and the speed of sound of DCE where already published by Valtz et al.³. In appendix, we have compared our experimental data with literature data.

For the DCE + MTBE, DCE + DIPE, DCE + DEE binary mixtures, the values of mixture densities and excess molar volumes are shown respectively in Table 3 to 5. The Redlich-Kister parameters and deviation for three binary systems are presented in **Erreur ! Source du renvoi introuvable.** to S3 (in supporting Information). The number of Redlich-Kister parameters is selected according to the method of Desnoyers and Perron¹⁶. At all temperatures, $v^E/x_1 x_2$ as a function of x_1 and v^E as a function of x_1 are represented, respectively, in Figure 1 and Figure 2 for the DCE + MTBE system, in Figure 3 and Figure 4 for the DCE + DIPE system, and in Figure 5 and Figure 6 for the DCE + DEE system.

Table 2: Experimental densities ρ_i and speed of sound u_i of the four compounds at different temperatures T and atmospheric pressure ($p = 101.33$ kPa).

T / K	DCE^a		DIPE		MTBE		DEE	
	$\rho / \text{kg.m}^{-3}$	$u / \text{m.s}^{-1}$	$\rho / \text{kg.m}^{-3}$	$u / \text{m.s}^{-1}$	$\rho / \text{kg.m}^{-3}$	$u / \text{m.s}^{-1}$	$\rho / \text{kg.m}^{-3}$	$u / \text{m.s}^{-1}$
278.14	1274.6	1271.2	739.1	1088.1	756.1	1128.9	730.8	1075.4
279.15	1273.2	1267.5	738.0	1083.8	755.1	1124.4	729.7	1070.9
280.15	1271.7	1263.3	737.0	1078.9	754.1	1119.3	728.6	1065.8
281.15	1270.3	1259.7	736.0	1074.7	753.0	1115.0	727.4	1061.4
282.15	1268.8	1255.4	735.0	1069.7	752.0	1109.8	726.3	1056.2
283.15	1267.4	1251.9	733.9	1065.5	751.0	1105.6	725.1	1051.8
284.15	1266.0	1247.6	732.9	1060.6	749.9	1100.4	724.0	1046.5
285.14	1264.5	1244.0	731.9	1056.4	748.9	1096.2	722.9	1042.2
286.15	1263.1	1239.7	730.9	1051.4	747.9	1090.9	721.7	1037.0
287.15	1261.6	1236.2	729.8	1047.3	746.9	1086.7	720.6	1032.6
288.15	1260.2	1231.8	728.8	1042.3	745.8	1081.5	719.4	1027.3
289.15	1258.7	1228.3	727.8	1038.2	744.8	1077.3	718.3	1023.0
290.15	1257.3	1224.0	726.7	1033.2	743.7	1072.0	717.1	1017.6
291.15	1255.8	1220.6	725.7	1029.2	742.7	1067.9	715.9	1013.5
292.15	1254.4	1216.2	724.7	1024.2	741.7	1062.8	714.8	1008.2
293.15	1252.9	1212.8	723.6	1020.3	740.6	1058.7	713.6	1004.0
294.15	1251.4	1208.5	722.6	1015.3	739.6	1053.6	712.4	998.7
295.15	1250.0	1205.1	721.5	1011.3	738.5	1049.5	711.2	994.5
296.15	1248.5	1200.7	720.5	1006.4	737.5	1044.3	710.1	989.2
297.14	1247.1	1197.3	719.5	1002.3	736.4	1040.1	708.9	984.9
298.15	1245.6	1193.0	718.4	997.7	735.4	1035.4	707.7	980.0
299.15	1244.2	1189.6	717.4	993.4	734.3	1030.8	706.5	975.4
300.15	1242.7	1185.6	716.3	988.9	733.3	1026.2	705.4	970.5
301.15	1241.2	1181.8	715.3	984.4	732.2	1021.5	704.2	965.7
302.15	1239.8	1177.9	714.2	980.0	731.1	1016.9	703.0	961.0
303.14	1238.3	1174.0	713.1	975.6	730.1	1012.3	701.8	956.2
304.14	1236.8	1170.2	712.1	971.1	729.0	1007.7	700.6	951.5
305.14	1235.4	1166.3	711.0	966.7	727.9	1003.0	699.4	946.8
306.15	1233.9	1162.4	710.0	962.2	726.9	998.4	698.2	942.0
307.15	1232.4	1158.6	708.9	957.8	725.8	993.8	697.0	937.3
308.15	1231.0	1155.1	707.8	953.4	724.7	989.2		
309.15	1229.5	1150.9	706.8	949.0	723.7	984.6		
310.15	1228.0	1147.1	705.7	944.6	722.6	980.0		
311.15	1226.5	1143.2	704.6	940.3	721.5	975.4		
312.15	1225.1	1139.4	703.6	935.9	720.4	970.8		
313.15	1223.6	1135.3	702.5	931.1	719.3	966.2		
314.15	1222.1	1131.7	701.4	927.2	718.2	961.6		
315.15	1220.6	1127.9	700.3	922.8	717.1	957.0		
316.15	1219.1	1124.1	699.3	918.4	716.1	952.5		
317.15	1217.6	1120.3	698.2	914.0	715.0	947.9		
318.15	1216.2	1116.2	697.1	909.3	713.9	943.1		
319.14	1214.7	1112.6	696.0	905.2	712.8	938.7		
320.15	1213.2	1108.8	694.9	900.8	711.7	934.1		
321.15	1211.7	1105.0	693.8	896.5	710.6	929.6		
322.15	1210.2	1101.2	692.7	892.2	709.4	925.0		
323.14	1208.7	1097.2	691.6	887.9	708.3	920.5		

324.15	1207.2	1093.6	690.5	883.6	707.2	915.9
325.15	1205.7	1089.8	689.4	879.2	706.1	911.4
326.14	1204.2	1086.0	688.3	874.9	705.0	906.9
327.15	1202.7	1082.2	687.2	870.6	703.9	902.4
328.14	1201.2	1078.2	686.1	866.3	702.7	897.9
329.15	1199.7	1074.6	685.0	862.0	701.6	893.4
330.14	1198.2	1070.9	683.9	857.7		
331.14	1196.7	1067.1	682.8	853.4		
332.15	1195.2	1063.3	681.7	849.1		
333.14	1193.7	1059.3	680.6	844.7		
334.14	1192.2	1055.7	679.4	840.4		
335.15	1190.6	1052.0	678.3	836.1		
336.15	1189.1	1048.2	677.2	831.8		
337.15	1187.6	1044.4	676.1	827.5		
338.15	1186.1	1040.6	674.9	823.3		
339.15	1184.6	1036.9	673.8	819.0		
340.14	1183.0	1033.2	672.7	814.8		
341.15	1181.5	1029.4	671.5	810.6		
342.14	1180.0	1025.6				

^a: These data were already published by Valtz et al. [3] in 2011

Standard uncertainty $u(p) = 0.1$ kPa, $u(T) = 0.01$ K

Expanded uncertainties ($k = 2$) $U(\rho_i) = 1.5$ kg.m⁻³, $U(u_i) = 0.5$ m.s⁻¹

Table 3: DCE (1) + MTBE (2) binary mixture densities ρ and excess molar volumes v^E as a function of mole fraction in DCE x_1 at different temperatures T and atmospheric pressure ($p = 101.33$ kPa).

$x_1 \backslash T / \text{K}$	278.15		283.15		288.15		293.15		298.15	
	$\rho / \text{kg.m}^{-3}$	$v^E / \text{cm}^3.\text{mol}^{-1}$	$\rho / \text{kg.m}^{-3}$	$v^E / \text{cm}^3.\text{mol}^{-1}$	$\rho / \text{kg.m}^{-3}$	$v^E / \text{cm}^3.\text{mol}^{-1}$	$\rho / \text{kg.m}^{-3}$	$v^E / \text{cm}^3.\text{mol}^{-1}$	$\rho / \text{kg.m}^{-3}$	$v^E / \text{cm}^3.\text{mol}^{-1}$
1.000	1274.6	0.000	1267.4	0.000	1260.2	0.000	1252.9	0.000	1245.6	0.000
0.975	1256.1	-0.043	1248.9	-0.045	1241.8	-0.047	1234.6	-0.050	1227.4	-0.051
0.950	1237.8	-0.078	1230.8	-0.082	1223.7	-0.085	1216.6	-0.089	1209.5	-0.093
0.900	1202.9	-0.150	1196.0	-0.157	1189.0	-0.164	1182.1	-0.170	1175.1	-0.178
0.859	1175.0	-0.205	1168.2	-0.213	1161.3	-0.223	1154.5	-0.233	1147.6	-0.243
0.800	1136.7	-0.272	1130.1	-0.284	1123.4	-0.297	1116.7	-0.309	1110.0	-0.323
0.749	1105.1	-0.329	1098.6	-0.343	1092.1	-0.358	1085.5	-0.373	1078.9	-0.390
0.700	1076.1	-0.371	1069.7	-0.388	1063.3	-0.406	1056.8	-0.422	1050.4	-0.441
0.650	1047.2	-0.413	1041.0	-0.431	1034.7	-0.449	1028.3	-0.468	1021.9	-0.488
0.600	1020.2	-0.453	1014.0	-0.473	1007.8	-0.492	1001.6	-0.511	995.3	-0.532
0.527	981.9	-0.502	975.9	-0.522	969.8	-0.543	963.7	-0.563	957.6	-0.586
0.500	968.4	-0.502	962.4	-0.523	956.4	-0.543	950.4	-0.562	944.3	-0.585
0.476	956.6	-0.520	950.7	-0.539	944.7	-0.560	938.7	-0.580	932.7	-0.604
0.450	944.0	-0.512	938.1	-0.533	932.2	-0.553	926.3	-0.573	920.3	-0.594
0.414	926.9	-0.522	921.1	-0.542	915.2	-0.563	909.3	-0.581	903.4	-0.604
0.350	897.4	-0.507	891.7	-0.525	886.0	-0.543	880.2	-0.561	874.4	-0.584
0.323	885.4	-0.509	879.8	-0.527	874.1	-0.545	868.4	-0.561	862.7	-0.584
0.250	853.9	-0.445	848.4	-0.462	842.9	-0.478	837.3	-0.491	831.7	-0.511
0.200	833.1	-0.390	827.7	-0.403	822.2	-0.415	816.7	-0.429	811.1	-0.446
0.150	813.0	-0.319	807.6	-0.331	802.2	-0.340	796.8	-0.350	791.3	-0.366
0.098	792.5	-0.226	787.2	-0.235	781.9	-0.242	776.6	-0.248	771.2	-0.258
0.050	774.5	-0.116	769.3	-0.120	764.1	-0.126	758.8	-0.127	753.5	-0.133
0.025	765.3	-0.063	760.1	-0.068	754.9	-0.071	749.7	-0.072	744.4	-0.077
0.000	756.1	0.000	751.0	0.000	745.8	0.000	740.6	0.000	735.4	0.000

Table 3 (continued)

T/K x_i	303.15		308.15		313.15		318.15		323.15	
	$\rho / \text{kg.m}^{-3}$	$v^E / \text{cm}^3.\text{mol}^{-1}$	$\rho / \text{kg.m}^{-3}$	$v^E / \text{cm}^3.\text{mol}^{-1}$	$\rho / \text{kg.m}^{-3}$	$v^E / \text{cm}^3.\text{mol}^{-1}$	$\rho / \text{kg.m}^{-3}$	$v^E / \text{cm}^3.\text{mol}^{-1}$	$\rho / \text{kg.m}^{-3}$	$v^E / \text{cm}^3.\text{mol}^{-1}$
1.000	1238.3	0.000	1231.0	0.000	1223.6	0.000	1216.2	0.000	1208.7	0.000
0.975	1220.2	-0.054	1212.9	-0.055	1205.6	-0.057	1198.2	-0.059	1190.8	-0.063
0.950	1202.3	-0.097	1195.1	-0.101	1187.8	-0.106	1180.6	-0.109	1173.3	-0.116
0.900	1168.0	-0.187	1161.0	-0.194	1153.9	-0.201	1146.7	-0.211	1139.6	-0.222
0.859	1140.7	-0.255	1133.7	-0.265	1126.7	-0.277	1119.7	-0.290	1112.6	-0.304
0.800	1103.2	-0.338	1096.4	-0.351	1089.5	-0.367	1082.7	-0.389	1075.7	-0.404
0.749	1072.2	-0.407	1065.5	-0.422	1058.8	-0.443	1052.1	-0.463	1045.3	-0.485
0.700	1043.8	-0.459	1037.2	-0.478	1030.6	-0.501	1024.0	-0.524	1017.3	-0.548
0.650	1015.5	-0.508	1009.1	-0.531	1002.6	-0.556	996.0	-0.580	989.4	-0.607
0.600	989.0	-0.554	982.6	-0.579	976.2	-0.604	969.8	-0.630	963.3	-0.658
0.527	951.4	-0.610	945.2	-0.634	939.0	-0.661	932.7	-0.688	926.3	-0.718
0.500	938.2	-0.610	932.0	-0.635	925.8	-0.661	919.6	-0.688	913.3	-0.719
0.476	926.7	-0.629	920.5	-0.652	914.4	-0.680	908.1	-0.704	901.9	-0.737
0.450	914.3	-0.619	908.2	-0.644	902.1	-0.671	895.9	-0.698	889.7	-0.728
0.414	897.5	-0.629	891.5	-0.653	885.4	-0.680	879.3	-0.707	873.2	-0.737
0.350	868.6	-0.607	862.7	-0.630	856.7	-0.655	850.7	-0.680	844.7	-0.708
0.323	856.9	-0.607	851.0	-0.628	845.1	-0.654	839.2	-0.679	833.2	-0.706
0.250	826.0	-0.531	820.3	-0.549	814.5	-0.572	808.6	-0.592	802.8	-0.616
0.200	805.5	-0.463	799.9	-0.478	794.2	-0.497	788.4	-0.516	782.6	-0.537
0.150	785.8	-0.379	780.3	-0.391	774.6	-0.407	768.9	-0.420	763.2	-0.436
0.098	765.7	-0.268	760.3	-0.276	754.7	-0.287	749.1	-0.298	743.5	-0.310
0.050	748.1	-0.140	742.7	-0.144	737.2	-0.151	731.7	-0.155	726.1	-0.163
0.025	739.1	-0.080	733.7	-0.080	728.3	-0.086	722.8	-0.088	717.2	-0.092
0.000	731.1	0.000	724.7	0.000	719.3	0.000	713.9	0.000	708.3	0.000

Standard uncertainty $u(p) = 0.1$ kPa, $u(T) = 0.01$ K, $u(x_i) = 0.002$

Expanded uncertainties ($k = 2$) $U(\rho) = 1.7$ g.cm⁻³, $U(v^E) = 0.011$ cm³.mol⁻¹

Table 4: DCE (1) + DIPE (2) binary mixture densities ρ and excess molar volumes v^E as a function of mole fraction in DCE x_1 at different temperatures T and atmospheric pressure ($p = 101.33$ kPa).

T/K x_1	283.15		288.15		293.15		298.15		303.15	
	$\rho / \text{kg.m}^{-3}$	$v^E / \text{cm}^3.\text{mol}^{-1}$	$\rho / \text{kg.m}^{-3}$	$v^E / \text{cm}^3.\text{mol}^{-1}$	$\rho / \text{kg.m}^{-3}$	$v^E / \text{cm}^3.\text{mol}^{-1}$	$\rho / \text{kg.m}^{-3}$	$v^E / \text{cm}^3.\text{mol}^{-1}$	$\rho / \text{kg.m}^{-3}$	$v^E / \text{cm}^3.\text{mol}^{-1}$
1.000	1267.4	0.000	1260.2	0.000	1252.9	0.000	1245.6	0.000	1238.3	0.000
0.980	1249.7	-0.082	1242.5	-0.084	1235.3	-0.086	1228.1	-0.088	1220.8	-0.090
0.960	1232.6	-0.136	1225.5	-0.141	1218.4	-0.144	1211.2	-0.147	1204.0	-0.150
0.940	1215.7	-0.187	1208.6	-0.192	1201.6	-0.198	1194.4	-0.200	1187.3	-0.206
0.920	1199.2	-0.235	1192.2	-0.242	1185.2	-0.249	1178.2	-0.255	1171.1	-0.260
0.900	1183.2	-0.285	1176.3	-0.293	1169.3	-0.300	1162.3	-0.307	1155.3	-0.313
0.850	1144.4	-0.382	1137.6	-0.393	1130.7	-0.403	1123.9	-0.413	1117.0	-0.424
0.800	1109.0	-0.487	1102.3	-0.500	1095.6	-0.512	1088.9	-0.524	1082.1	-0.536
0.750	1075.1	-0.567	1068.5	-0.581	1062.0	-0.596	1055.3	-0.610	1048.7	-0.625
0.690	1037.0	-0.662	1030.6	-0.678	1024.2	-0.695	1017.7	-0.711	1011.2	-0.726
0.650	1013.1	-0.693	1006.8	-0.711	1000.5	-0.727	994.1	-0.744	987.6	-0.758
0.600	984.7	-0.741	978.5	-0.758	972.3	-0.775	966.0	-0.793	959.7	-0.811
0.550	957.8	-0.755	951.7	-0.775	945.6	-0.791	939.4	-0.806	933.2	-0.825
0.500	932.3	-0.779	926.3	-0.798	920.3	-0.812	914.2	-0.827	908.1	-0.845
0.450	908.1	-0.778	902.2	-0.794	896.2	-0.810	890.2	-0.827	884.2	-0.844
0.400	885.0	-0.761	879.2	-0.777	873.3	-0.793	867.4	-0.808	861.5	-0.823
0.350	863.0	-0.729	857.3	-0.748	851.5	-0.762	845.7	-0.774	839.9	-0.788
0.300	842.1	-0.679	836.4	-0.694	830.8	-0.707	825.1	-0.723	819.3	-0.735
0.250	822.1	-0.627	816.6	-0.639	811.0	-0.649	805.4	-0.659	799.7	-0.672
0.200	802.9	-0.528	797.4	-0.538	791.9	-0.547	786.4	-0.557	780.8	-0.568
0.150	784.5	-0.414	779.1	-0.421	773.7	-0.427	768.2	-0.435	762.7	-0.444
0.100	767.0	-0.297	761.7	-0.307	756.3	-0.312	751.0	-0.315	745.5	-0.321
0.080	760.1	-0.237	754.8	-0.244	749.5	-0.247	744.2	-0.250	738.8	-0.254
0.060	753.4	-0.177	748.1	-0.182	742.9	-0.188	737.6	-0.190	732.2	-0.199
0.040	746.7	-0.100	741.5	-0.106	736.2	-0.106	731.0	-0.107	725.6	-0.109
0.020	740.2	-0.042	735.0	-0.046	729.8	-0.047	724.6	-0.046	719.3	-0.047
0.000	733.9	0.000	728.8	0.000	723.6	0.000	718.4	0.000	713.1	0.000

Table 4 (continued)

T/K x_1	308.15		313.15		318.15		323.15		328.15		333.15	
	$\rho / \text{kg.m}^{-3}$	$v^E / \text{cm}^3.\text{mol}^{-1}$	$\rho / \text{kg.m}^{-3}$	$v^E / \text{cm}^3.\text{mol}^{-1}$	$\rho / \text{kg.m}^{-3}$	$v^E / \text{cm}^3.\text{mol}^{-1}$	$\rho / \text{kg.m}^{-3}$	$v^E / \text{cm}^3.\text{mol}^{-1}$	$\rho / \text{kg.m}^{-3}$	$v^E / \text{cm}^3.\text{mol}^{-1}$	$\rho / \text{kg.m}^{-3}$	$v^E / \text{cm}^3.\text{mol}^{-1}$
1.000	1231.0	0.000	1223.6	0.000	1216.2	0.000	1208.7	0.000	1201.2	0.000	1193.7	0.000
0.980	1213.5	-0.091	1206.2	-0.093	1198.9	-0.094	1191.5	-0.097	1184.0	-0.099	1176.5	-0.103
0.960	1196.8	-0.154	1189.5	-0.158	1182.2	-0.163	1174.9	-0.167	1167.5	-0.170	1160.0	-0.176
0.940	1180.1	-0.210	1172.9	-0.215	1165.7	-0.221	1158.4	-0.227	1151.0	-0.234	1143.7	-0.241
0.920	1163.9	-0.267	1156.8	-0.274	1149.6	-0.282	1142.4	-0.290	1135.1	-0.297	1127.8	-0.307
0.900	1148.2	-0.321	1141.1	-0.331	1134.0	-0.339	1126.8	-0.350	1119.6	-0.360	1112.3	-0.371
0.850	1110.1	-0.435	1103.1	-0.448	1096.1	-0.461	1089.1	-0.474	1082.0	-0.487	1074.8	-0.502
0.800	1075.3	-0.551	1068.5	-0.566	1061.6	-0.582	1054.7	-0.599	1047.7	-0.615	1040.7	-0.634
0.750	1042.0	-0.640	1035.3	-0.656	1028.5	-0.673	1021.7	-0.693	1014.8	-0.712	1007.9	-0.734
0.690	1004.7	-0.744	998.1	-0.764	991.4	-0.784	984.8	-0.805	978.0	-0.827	971.3	-0.851
0.650	981.2	-0.777	974.7	-0.798	968.1	-0.819	961.5	-0.841	954.9	-0.865	948.2	-0.889
0.600	953.3	-0.830	947.0	-0.851	940.5	-0.872	934.0	-0.895	927.5	-0.921	920.9	-0.945
0.550	926.9	-0.845	920.6	-0.866	914.3	-0.889	907.9	-0.912	901.5	-0.935	895.0	-0.959
0.500	901.9	-0.865	895.7	-0.886	889.5	-0.908	883.2	-0.930	876.8	-0.955	870.4	-0.980
0.450	878.1	-0.863	872.0	-0.884	865.9	-0.905	859.7	-0.928	853.4	-0.951	847.1	-0.974
0.400	855.5	-0.842	849.5	-0.861	843.5	-0.881	837.4	-0.901	831.2	-0.924	825.0	-0.945
0.350	834.0	-0.805	828.1	-0.824	822.1	-0.842	816.1	-0.861	810.0	-0.881	803.8	-0.900
0.300	813.5	-0.751	807.7	-0.768	801.8	-0.784	795.9	-0.801	789.9	-0.820	783.8	-0.839
0.250	794.0	-0.686	788.2	-0.700	782.4	-0.715	776.6	-0.733	770.7	-0.749	764.7	-0.765
0.200	775.2	-0.580	769.5	-0.591	763.8	-0.603	758.0	-0.617	752.2	-0.631	746.3	-0.643
0.150	757.2	-0.459	751.6	-0.464	746.0	-0.474	740.3	-0.485	734.6	-0.495	728.8	-0.505
0.100	740.1	-0.328	734.6	-0.336	729.0	-0.343	723.4	-0.351	717.8	-0.357	712.0	-0.362
0.080	733.4	-0.259	727.9	-0.267	722.4	-0.273	716.8	-0.278	711.2	-0.284	705.5	-0.288
0.060	726.8	-0.196	721.4	-0.200	715.9	-0.205	710.3	-0.209	704.7	-0.214	699.1	-0.215
0.040	720.3	-0.113	714.9	-0.116	709.4	-0.121	703.9	-0.124	698.3	-0.127	692.7	-0.126
0.020	714.0	-0.050	708.6	-0.051	703.2	-0.055	697.7	-0.056	692.1	-0.057	686.5	-0.057
0.000	707.8	0.000	702.5	0.000	697.1	0.000	691.6	0.000	686.1	0.000	680.6	0.000

Standard uncertainty $u(p) = 0.1 \text{ kPa}$, $u(T) = 0.01 \text{ K}$, $u(x_1) = 0.002$ Expanded uncertainties ($k = 2$) $U(\rho) = 1.7 \text{ kg.m}^{-3}$, $U(v^E) = 0.011 \text{ cm}^3.\text{mol}^{-1}$

Table 5: DCE (1) + DEE (2) binary mixture densities ρ and excess molar volumes v^E as a function of mole fraction in DCE x_1 at different temperatures T and atmospheric pressure ($p = 101.33$ kPa)..

T / K	283.15		288.15		293.15		298.15		303.15		308.15	
	x_1	$\rho / \text{kg.m}^{-3}$	$v^E / \text{cm}^3.\text{mol}^{-1}$	$\rho / \text{kg.m}^{-3}$	$v^E / \text{cm}^3.\text{mol}^{-1}$	$\rho / \text{kg.m}^{-3}$	$v^E / \text{cm}^3.\text{mol}^{-1}$	$\rho / \text{kg.m}^{-3}$	$v^E / \text{cm}^3.\text{mol}^{-1}$	$\rho / \text{kg.m}^{-3}$	$v^E / \text{cm}^3.\text{mol}^{-1}$	$\rho / \text{kg.m}^{-3}$
1.000	1267.4	0.000	1260.2	0.000	1252.9	0.000	1245.6	0.000	1238.3	0.000	1231.0	0.000
0.980	1254.4	-0.065	1247.2	-0.068	1240.0	-0.070	1232.7	-0.073	1225.4	-0.077	1218.1	-0.079
0.960	1241.2	-0.121	1234.0	-0.127	1226.8	-0.133	1219.6	-0.138	1212.4	-0.144	1205.1	-0.148
0.940	1228.5	-0.172	1221.4	-0.179	1214.2	-0.187	1207.0	-0.194	1199.8	-0.203	1192.6	-0.212
0.915	1211.5	-0.217	1204.5	-0.228	1197.3	-0.237	1190.2	-0.246	1183.0	-0.258	1175.8	-0.269
0.898	1200.8	-0.253	1193.8	-0.265	1186.7	-0.277	1179.6	-0.291	1172.4	-0.300	1165.2	-0.313
0.850	1170.5	-0.353	1163.5	-0.369	1156.5	-0.385	1149.4	-0.402	1142.4	-0.419	1135.2	-0.439
0.798	1138.3	-0.449	1131.4	-0.468	1124.4	-0.489	1117.5	-0.510	1110.4	-0.533	1103.4	-0.557
0.750	1109.8	-0.545	1103.0	-0.567	1096.2	-0.592	1089.3	-0.618	1082.3	-0.645	1075.3	-0.675
0.699	1079.4	-0.613	1072.7	-0.639	1065.9	-0.667	1059.1	-0.696	1052.2	-0.727	1045.3	-0.760
0.649	1050.7	-0.662	1044.0	-0.690	1037.3	-0.720	1030.5	-0.752	1023.7	-0.784	1016.8	-0.820
0.600	1023.2	-0.733	1016.6	-0.763	1010.0	-0.796	1003.3	-0.829	996.5	-0.863	989.7	-0.902
0.550	995.5	-0.765	988.9	-0.795	982.3	-0.828	975.7	-0.865	969.0	-0.901	962.3	-0.942
0.500	968.7	-0.813	962.2	-0.844	955.7	-0.877	949.2	-0.914	942.5	-0.952	935.9	-0.994
0.450	942.2	-0.816	935.8	-0.848	929.3	-0.882	922.8	-0.919	916.3	-0.957	909.7	-0.998
0.400	916.2	-0.816	909.9	-0.847	903.5	-0.880	897.1	-0.923	890.6	-0.954	884.1	-0.996
0.350	890.7	-0.783	884.5	-0.813	878.2	-0.846	871.8	-0.881	865.4	-0.917	858.9	-0.958
0.300	865.7	-0.741	859.6	-0.768	853.3	-0.799	847.0	-0.834	840.7	-0.865	834.3	-0.905
0.250	841.3	-0.688	835.2	-0.712	829.0	-0.741	822.9	-0.782	816.5	-0.801	810.2	-0.837
0.200	817.2	-0.598	811.1	-0.618	805.0	-0.644	798.9	-0.671	792.7	-0.698	786.4	-0.730
0.150	793.5	-0.484	787.5	-0.499	781.5	-0.520	775.4	-0.544	769.3	-0.567	763.1	-0.595
0.100	770.2	-0.344	764.4	-0.358	758.4	-0.374	752.4	-0.391	746.3	-0.406	740.2	-0.425
0.080	761.1	-0.288	755.3	-0.297	749.4	-0.310	743.5	-0.339	737.4	-0.338	731.2	-0.354
0.065	754.3	-0.237	748.5	-0.248	742.6	-0.262	736.6	-0.272	730.6	-0.282	724.5	-0.296
0.050	747.5	-0.184	741.7	-0.193	735.8	-0.205	729.9	-0.217	723.9	-0.220	717.8	-0.230
0.040	743.0	-0.150	737.2	-0.157	731.3	-0.167	725.4	-0.177	719.4	-0.182	713.4	-0.192
0.020	734.0	-0.069	728.2	-0.071	722.4	-0.077	716.5	-0.083	710.5	-0.086	704.5	-0.091
0.000	725.1	0.000	719.4	0.000	713.6	0.000	707.7	0.000	701.8	0.000	695.8	0.000

Standard uncertainty $u(p) = 0.1$ kPa, $u(T) = 0.01$ K, $u(x_i) = 0.002$

Expanded uncertainties ($k = 2$) $U(\rho) = 1.7$ kg.m⁻³, $U(v^E) = 0.011$ cm³.mol⁻¹

Table 6: PFP parameters: molar volume V_i , thermal expansion coefficient α_i , liquid heat capacity C_{pi} , isentropic compressibility κ_{si} , isothermal compressibility κ_{Ti} , and their standard deviations $u(x)$ for DCE.

PFP Parameter	a	$u(a)$	b	$u(b)$	c	$u(c)$
$V_i/\text{cm}^3\cdot\text{mol}^{-1}$	0.000149	0.000001	0.00429	0.00053	64.9	0.1
$10^5 \alpha_i/\text{K}^{-1}$	-0.000498	0.000001	0.535	0.001	2.18	0.01
$C_{pi}/\text{J}\cdot\text{mol}^{-1}\cdot\text{K}^{-1}$	0.00036	0.00003	-0.140	0.016	138.0	2.6
$10^9 \kappa_{si}/\text{Pa}^{-1}$	0.0000228	0.0000003	-0.0093	0.0002	1.29	0.02
$10^9 \kappa_{Ti}/\text{Pa}^{-1}$	0.0000258	0.0000003	-0.0090	0.0002	1.21	0.02

Table 7: PFP parameters: molar volume V_i , thermal expansion coefficient α_i , liquid heat capacity C_{pi} , isentropic compressibility κ_{si} , isothermal compressibility κ_{Ti} , and their standard deviations $u(x)$ for MTBE.

PFP Parameter	a	$u(a)$	b	$u(b)$	c	$u(c)$
$V_i/\text{cm}^3\cdot\text{mol}^{-1}$	0.000423	0.000003	-0.0798	0.0002	106.1	0.1
$10^3 \alpha_i/\text{K}^{-1}$	-0.0000122	0.0000001	0.0123	0.0001	-1.14	0.01
$C_{pi}/\text{J}\cdot\text{mol}^{-1}\cdot\text{K}^{-1}$	0.000444	0.000002	0.040	0.001	137.98	0.01
$10^9 \kappa_{si}/\text{Pa}^{-1}$	0.0000986	0.0000001	-0.0454	0.0008	6.05	0.01
$10^9 \kappa_{Ti}/\text{Pa}^{-1}$	0.000105	0.000001	-0.0455	0.0007	5.87	0.01

Table 8: PFP parameters: molar volume V_i , thermal expansion coefficient α_i , liquid heat capacity C_{pi} , isentropic compressibility κ_{si} , isothermal compressibility κ_{Ti} , and their standard deviations $u(x)$ for DIPE.

PFP Parameter	a	$u(a)$	b	$u(b)$	c	$u(c)$
$V_i/\text{cm}^3\cdot\text{mol}^{-1}$	0.000521	0.000004	-0.1032	0.0002	126.7	0.1
$10^3 \alpha_i/\text{K}^{-1}$	-0.0000129	0.0000001	0.0129	0.0001	-1.24	-0.01
$C_{pi}/\text{J}\cdot\text{mol}^{-1}\cdot\text{K}^{-1}$	-0.00049	0.00007	0.70	0.04	50.23	0.01
$10^9 \kappa_{si}/\text{Pa}^{-1}$	0.000121	0.000001	-0.0574	0.0009	7.78	0.01
$10^9 \kappa_{Ti}/\text{Pa}^{-1}$	0.000129	0.000001	-0.0582	0.0009	7.69	0.01

Table 9: PFP parameters: molar volume V_i , thermal expansion coefficient α_i , liquid heat capacity C_{pi} , isentropic compressibility κ_{si} , isothermal compressibility κ_{Ti} , and their standard deviations $u(x)$ for DEE.

PFP Parameter	a	$u(a)$	b	$u(b)$	c	$u(c)$
$V_i/\text{cm}^3\cdot\text{mol}^{-1}$	0.00048	0.00003	-0.108	0.001	94.7	0.2
$10^3 \alpha_i/\text{K}^{-1}$	-0.000018	0.0000004	0.0170	0.0001	-1.80	0.01
$C_{pi}/\text{J}\cdot\text{mol}^{-1}\cdot\text{K}^{-1}$	0.00008	0.00003	0.14	0.02	124	2
$10^9 \kappa_{si}/\text{Pa}^{-1}$	0.000118	0.000002	-0.054	0.001	7.0	0.2
$10^9 \kappa_{Ti}/\text{Pa}^{-1}$	0.000132	0.000002	-0.056	0.001	7.0	0.1

Table 6: Flory parameters χ_{12}^0 , d and e for the three systems DCE + ether at temperature T from 278.15 to 333.15 K.

T/K	DCE + MTBE			DCE + DIPE			DCE + DEE		
	$\chi_{12}^0/\text{J.cm}^{-3}$	d	e	$\chi_{12}^0/\text{J.cm}^{-3}$	d	e	$\chi_{12}^0/\text{J.cm}^{-3}$	d	e
278.15	-12.399	0.858	-0.661						
283.15	-11.454	0.850	-0.696	-16.640	1.012	0.042	-10.359	0.929	-0.377
288.15	-10.501	0.843	-0.723	-15.098	1.014	0.051	-9.020	0.929	-0.377
293.15	-9.436	0.835	-0.756	-13.444	1.020	0.070	-7.893	0.914	-0.445
298.15	-8.684	0.822	-0.811	-11.795	1.026	0.092	-7.016	0.894	-0.540
303.15	-7.954	0.811	-0.860	-10.245	1.032	0.113	-5.847	0.890	-0.550
308.15	-7.175	0.799	-0.906	-8.870	1.039	0.138	-5.128	0.876	-0.615
313.15	-6.600	0.789	-0.946	-7.572	1.054	0.189			
318.15	-6.014	0.784	-0.962	-6.367	1.072	0.251			
323.15	-5.594	0.777	-0.988	-5.267	1.100	0.342			
328.15				-4.253	1.137	0.469			
333.15				-3.294	1.214	0.727			

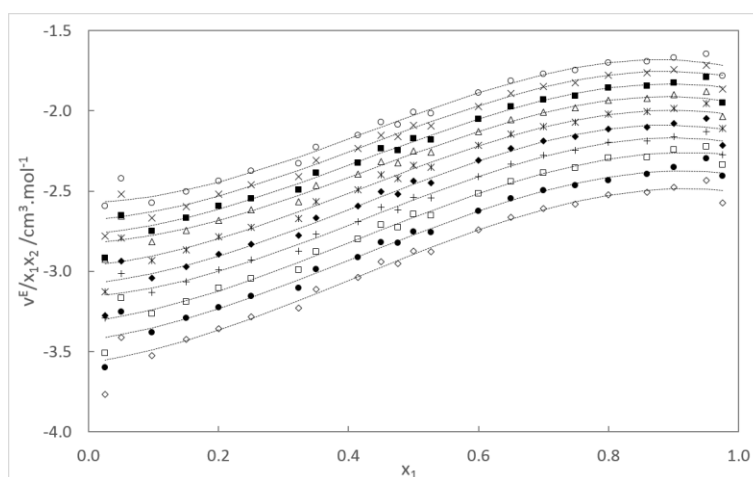


Figure 1: v^E/x_1x_2 for DCE (1) + MTBE (2) mixture according to x_1 different temperatures: \circ : 278 K, \times : 283 K, \blacksquare : 288 K, \triangle : 293 K, $*$: 298 K, \blacklozenge : 303 K, $+$: 308 K, \square : 313 K, \bullet : 318 K, \diamond : 323 K, \cdots : Redlich-Kister correlation.

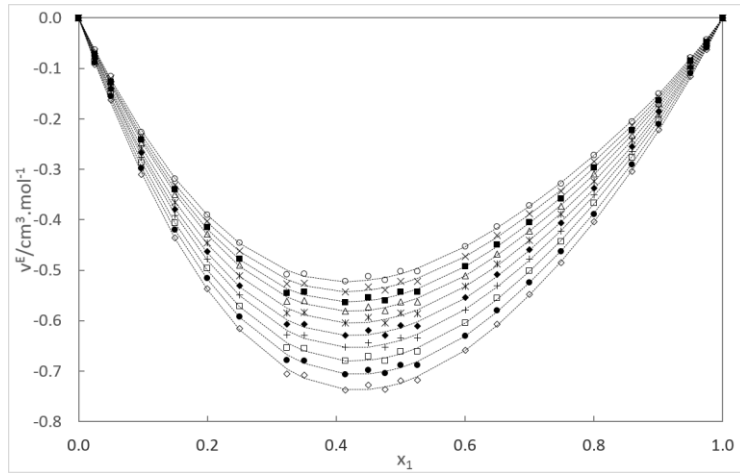


Figure 2: v^E for DCE (1) + MTBE (2) mixture according to x_1 different temperatures: \circ : 278 K, \times : 283 K, \blacksquare : 288 K, \triangle : 293 K, $*$: 298 K, \blacklozenge : 303 K, $+$: 308 K, \square : 313 K, \bullet : 318 K, \diamond : 323 K, \cdots : Redlich-Kister correlation.

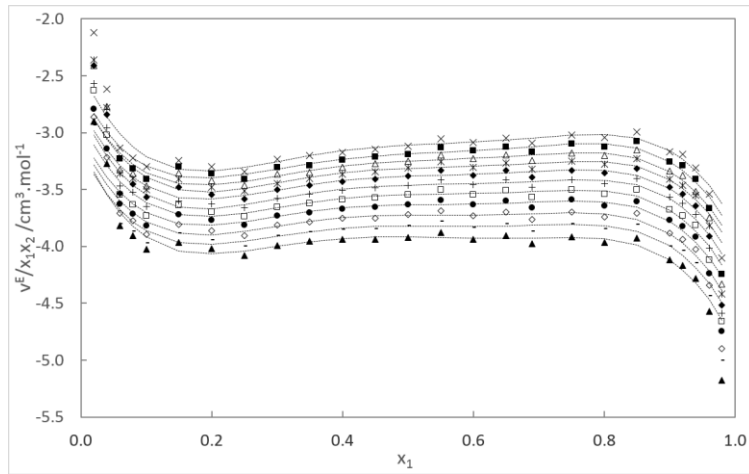


Figure 3: v^E/x_1x_2 for DCE (1) + DIPE (2) mixture according to x_1 at different temperatures: \times : 283 K, \blacksquare : 288 K, \triangle : 293 K, $*$: 298 K, \blacklozenge : 303 K, $+$: 308 K, \square : 313 K, \bullet : 318 K, \diamond : 323 K, $-$: 328 K, \blacktriangle : 333 K, \cdots : Redlich-Kister correlation.

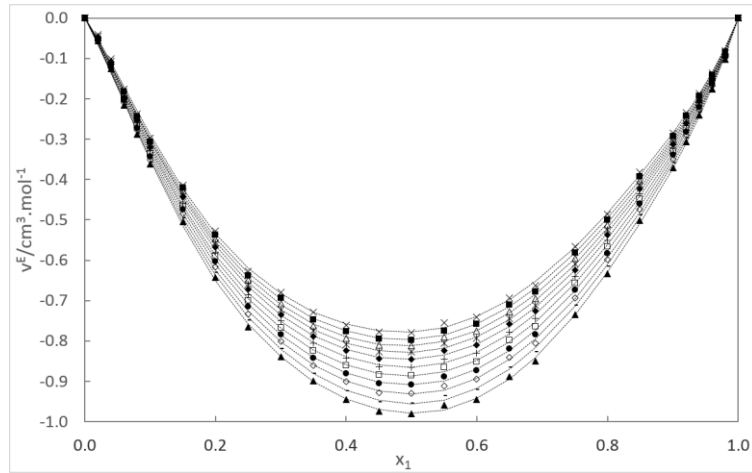


Figure 4: v^E for DCE (1) + DIPE (2) mixture according to x_1 at different temperatures: \times : 283 K, \blacksquare : 288 K, Δ : 293 K, $*$: 298 K, \blacklozenge : 303 K, $+$: 308 K, \square : 313 K, \bullet : 318 K, \diamond : 323 K, $-$: 328 K, \blacktriangle : 333 K, \cdots : Redlich-Kister correlation.

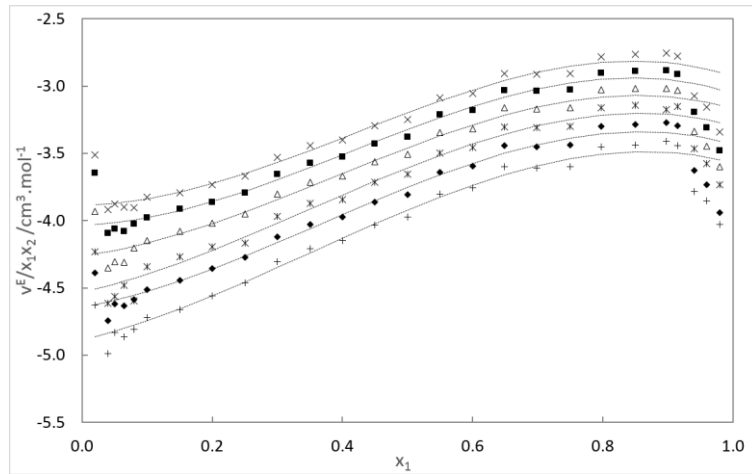


Figure 5: v^E/x_1x_2 for DCE (1) + DEE (2) mixture according to x_1 at different temperatures: \times : 283 K, \blacksquare : 288 K, Δ : 293 K, $*$: 298 K, \blacklozenge : 303 K, $+$: 308 K, \cdots : Redlich-Kister correlation.

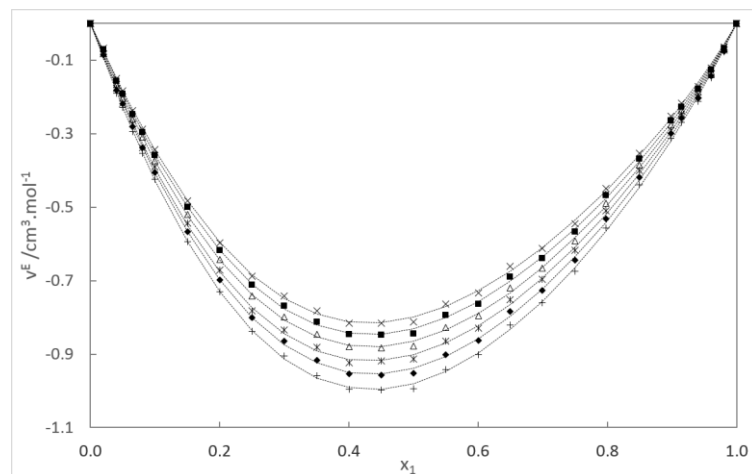


Figure 6: v^E for DCE (1) + DEE (2) mixture according to x_1 at different temperatures: \times : 283 K, \blacksquare : 288 K, Δ : 293 K, $*$: 298 K, \blacklozenge : 303 K, $+$: 308 K, \cdots : Redlich-Kister correlation.

To the best of our knowledge, no data from the literature, on the DCE + DEE and DCE + DIPE binary systems, was found. One study for the DCE + MTBE binary system was reported in the literature, by Sharma and al.¹⁷ at 303 K. A comparison of the two isotherms is presented in Figure 7. We can observe a good agreement between our data and the literature data, v^E as a function of x_1 follows the same trend.

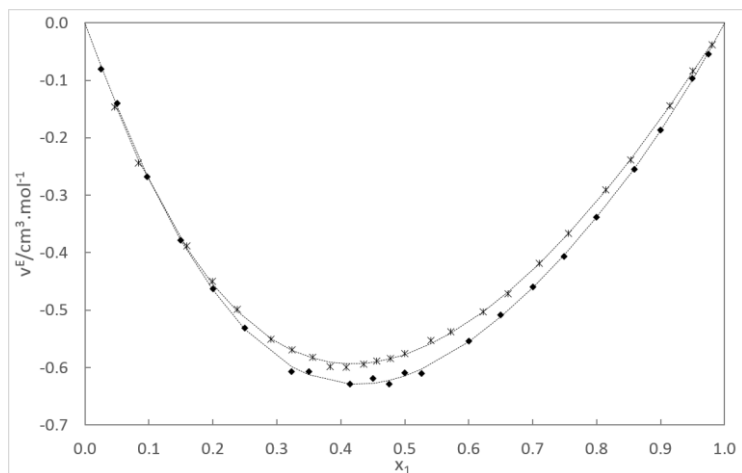


Figure 7: v^E for DCE (1) + MTBE (2) mixture according to x_1 at 303 K: \times : experimental data from Sharma and al.¹⁷, \blacklozenge : our experimental data, \cdots : Redlich-Kister correlation.

5. Discussion

Excess molar volume

The excess molar volumes are negative for the three binary systems, as we can see in Figure 2 to 6. and we can see that the amplitude increase with the temperature. The negative v^E for the three systems can be interpreted by the packing effect: a good insertion of the DCE molecule in the ethers or by a dipole-dipole interaction as the dipoles moments of the compounds are closed (DCE: 1.439 D, MTBE: 1.361 D, DIPE: 1.302 D and DEE: 1.151 D, data from Simulis Thermodynamics™ from PROSIM, France). The v^E values are symmetrical for the DCE + DEE and DCE + DIPE binary systems and slightly asymmetrical for the DCE + MTBE system. The maximal absolute v^E (at $x = 0.5$), over the entire temperature range, increases for the three binary systems with the temperature. At 298 K, the maximal absolute v^E for the DCE + MTBE, DCE + DIPE and DCE + DEE systems are respectively 0.586, 0.827 and 0.919. This amplitude difference between the three systems is due to the steric hindrance of the ether. When the ether molecule has a lower steric hindrance, it is better packed with the DCE molecule.

Following the method of Desnoyers and Perron¹⁶, v^E/x_1x_2 as a function of x_1 was also plotted for each binary systems, in Figure 1, Figure 3 and Figure 5. This term is directly related to the apparent molar volume following Eq. 23:

$$\frac{v^E}{x_1x_2} = \frac{v_{\phi_1} - v_1^0}{x_1} = \frac{v_{\phi_2} - v_2^0}{x_2} \quad 23$$

These graphics don't show any particular behavior relating to the behavior of the studied systems, in the diluted areas. The utilization of a polynomial expression like the one suggested by Redlich-Kister is not well-adapted for the representation of the excess volume for our three systems in the diluted areas. In effect, a good representation of excess volume requires a lot of parameters and can lead to a bad representation of the derivative properties. It is for this reason that we have also

considered another approach by considering the partial molar volume, obtained by derivative of the volume versus the mole number.

The apparent molar volumes of DCE in ether calculated from experimental data with Eq 11, and the partial molar volumes of DCE in ether estimated using the Redlich-Kister parameters A_n (Eq 8) for the three systems as a function of the DCE molar fraction x_1 are respectively presented in Figure 8 to 10 at two temperatures.

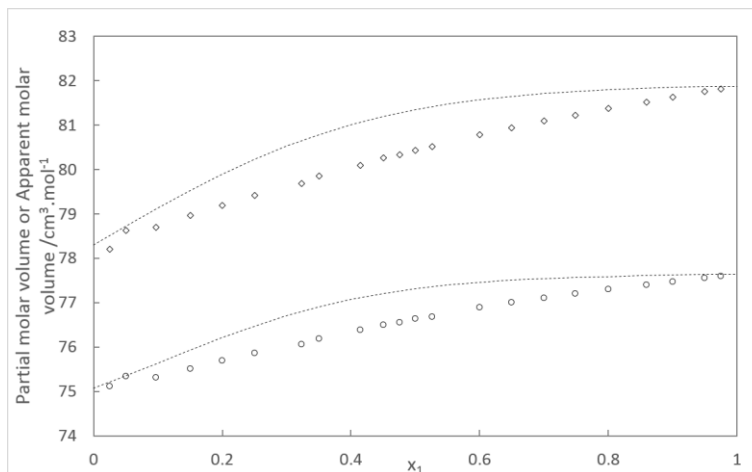


Figure 8: Apparent molar volume of DCE in the DCE + MTBE mixture according to x_1 at two temperatures: \circ : 278 K, \diamond : 323 K, \cdots : Estimated partial molar volume (from Eq. 8).

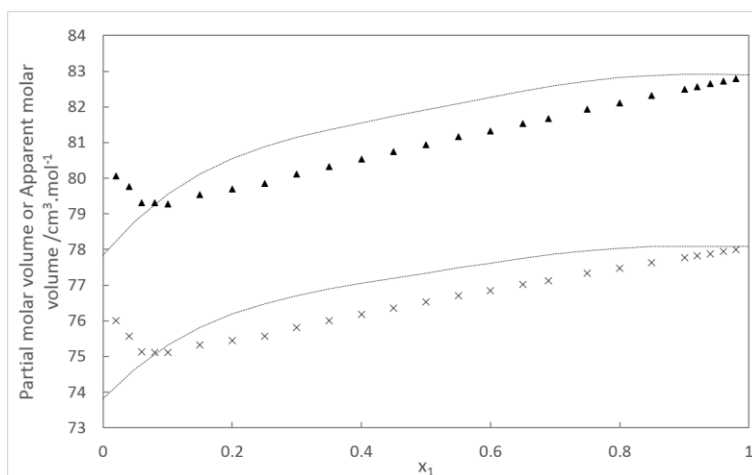


Figure 9: Apparent molar volume of DCE in the DCE + DIPE mixture according to x_1 at two temperatures: \times : 283 K, \blacktriangle : 333 K, \cdots : Estimated partial molar volume (from Eq. 8).

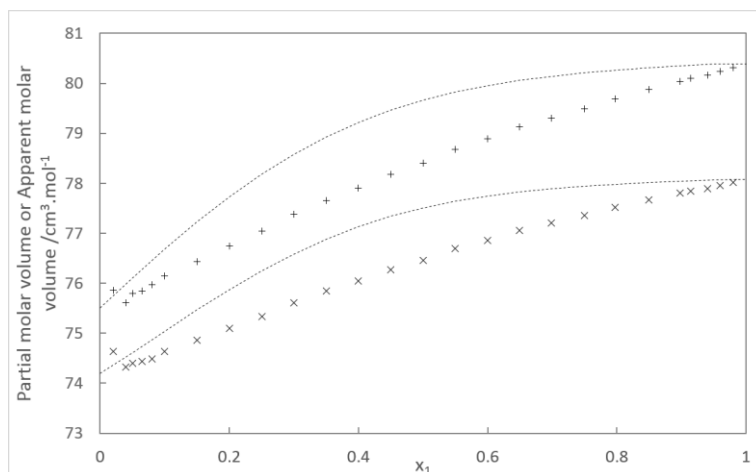


Figure 10: Apparent molar volume of DCE in the DCE + DEE mixture according to x_1 at two temperatures: \times : 283 K, $+$: 308 K, \cdots : Estimated partial molar volume (from Eq. 8).

The partial molar volume corresponds to the volume occupied by the solute in the solution. At infinite dilution, the main molecular interactions in the mixture are the solute-solvent and solvent-solvent interactions. It is an important property as it is linked to the nature of the molecular interaction between the solute and the solvent. As it can be seen in Figure 8 to 10, the results obtained using both approaches do not always agree, especially for the binary systems DCE + DEE and DCE + DIPE for regions with low DCE molar fraction. More information is needed in the very dilute region. Lastly, we have considered the Prigogine-Flory-Patterson (PFP) model for the data treatment.

Prigogine-Flory-Patterson model

To apply the PFP theory to our experimental data, we need to estimate several properties of the different molecules, such as the isothermal and isentropic compressibility κ_{Ti} and κ_{Si} , the molar volume V_i and the thermal expansion coefficient α_i . The experimental densities and speed of sound of the four compounds at different temperatures used to calculate the isentropic compressibility are presented in Table 2. The experimental liquid heat capacities, C_{pi} , measured by Goralski and al.¹⁸ are the ones used for the DCE pure compound. For the MTBE constituent, the values predicted by REFPROP¹⁹ are used. For the DIPE molecule, we have used the data from Paramo and al.²⁰. And for the DEE, we have used the data from Counsell and al.²¹.

The thermodynamics equations presented in section 0, are used to calculate these properties. The hypothesis that these properties can be expressed by a polynomial equation of the second-degree dependant on the temperature defined by Eq. 24, in our experimental conditions of temperature and pressure, was made.

$$F(T) = aT^2 + bT + c \quad 24$$

The parameters for the application of the PFP theory for the DCE, MTBE, DIPE, and DEE compound and their standard deviation, $u(x)$, are presented respectively in Table 6 to 9.

To treat the experimental with the PFP method, the χ_{12} parameter is regressed to minimize the objective function, F_C , defined in Eq. 25. The PFP parameters presented in Table 6 to 9 are used, according to the temperature.

$$Fc = \sum_i (v_{exp}^E - v_{PFP}^E)^2 \quad 25$$

As suggested by Coquelet and al.¹⁴, and applied by Ali Raza et al.²² we have also considered that the χ_{12} parameter is dependent on the composition of the solution following Eq. 26.

$$\chi_{12} = \chi_{12}^0(d + e(\varphi_1 - \varphi_2)) \quad 26$$

where the Flory parameter χ_{12}^0 is estimated independently of the composition.

The PFP model is used on the experimental data for the three binary systems and at all the temperatures. The χ_{12}^0 , d and e parameters (from Eq. 26) estimated with the objective function, Fc, are presented in Table 10. To compare the dependence or independence of the Flory parameter to the composition, the two PFP treatments for the three binary systems, respectively DCE + MTBE, DCE + DIPE, and DCE + DEE, at the lowest and the highest temperature of the experimental conditions, are presented in Figure 11 to 13. Consequently, we can see that the PFP model with a Flory parameter dependent on the composition represents better the excess molar volume estimated from the experimental data, especially for the DCE + MTBE mixture.

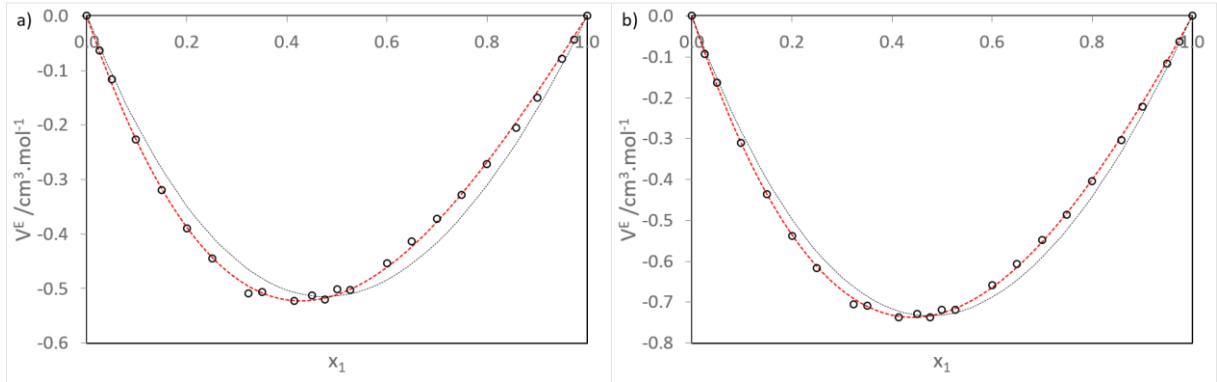


Figure 11: v^E for DCE (1) + MTBE (2) system according to x_1 ---: PFP model with χ_{12} parameter independent of the composition and ---: PFP model with χ_{12} parameter dependent of the composition; a) $T = 278$ K and b) $T = 323$ K.

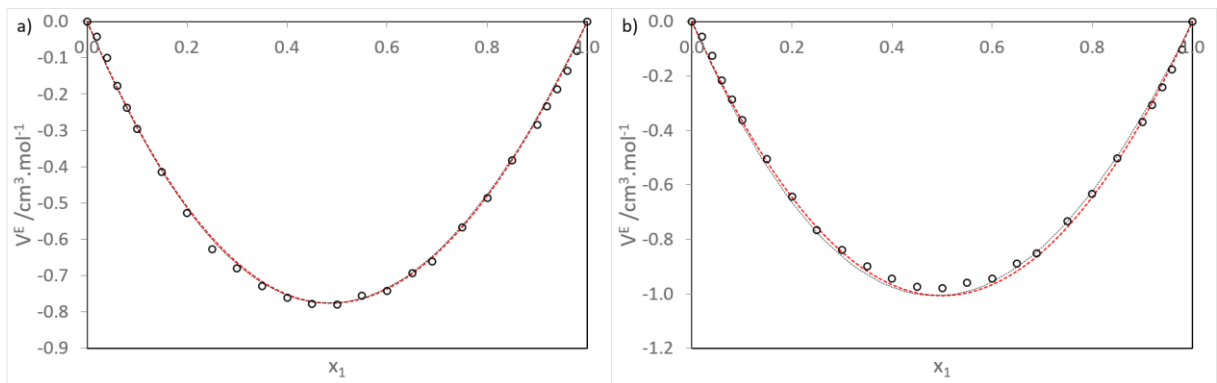


Figure 12: v^E for DCE (1) + DIPE (2) system according to x_1 ---: PFP model with χ_{12} parameter independent of the composition and ---: PFP model with χ_{12} parameter dependent of the composition; a) $T = 283$ K and b) $T = 333$ K.

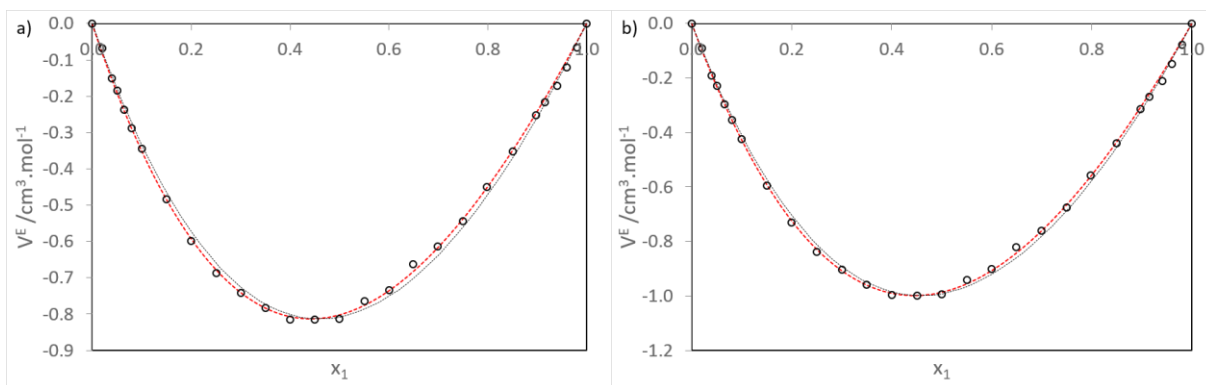


Figure 13: v^E for DCE (1) + DEE (2) system according to x_1 ---: PFP model with χ_{12} parameter independent of the composition and ---: PFP model with χ_{12} parameter dependent of the composition; a) $T = 283$ K and b) $T = 308$ K.

With the PFP model, we can also analyze the weight of the three contributions v_{int} , v_{fv} and v_{p^*} on the excess molar volume. In Figure 14 to 16, for three different temperatures of each binary system, the estimation with the PFP model of the three contributions according to the molar fraction of DCE is represented. For the DCE + MTBE mixture, the effect of the free volume contribution seems to slightly increase with the temperature and is less important than the other two. Moreover, the internal pressure is the main contributor to the excess molar volume, it increases when the temperature increases. The interactional contribution is also important at low temperature but it decreases when the temperature increases to the point where it has less impact than the v_{fv} . The observations are the same for the DCE + DIPE binary system. For the DCE + DEE binary mixture, the observations are also similar, nevertheless, the interactional contribution is no more significant, as the free volume contribution, at low temperatures. To the best of our knowledge, the only PFP treatment of any of the binary systems studied was the one on the DCE + MTBE binary system reported by Sharma and al.¹⁷ at 303 K. They also found, like us, that the P^* interaction is the main contribution to the excess molar volume of the mixture.

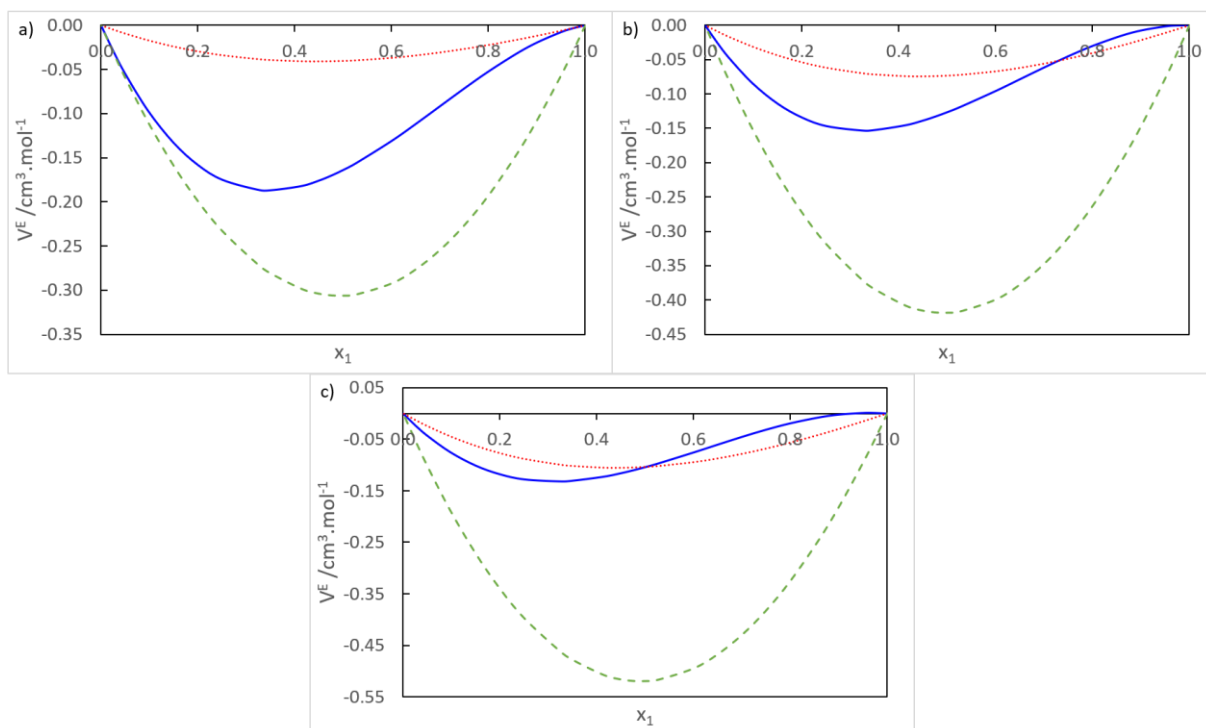


Figure 14: PFP contributions to v^E for DCE (1) + MTBE (2) system according to x_1 ; —: v_{int} , ...: v_{fv} , --: v_{P^*} ; a) $T = 278$ K, b) $T = 308$ K and c) $T = 323$ K.

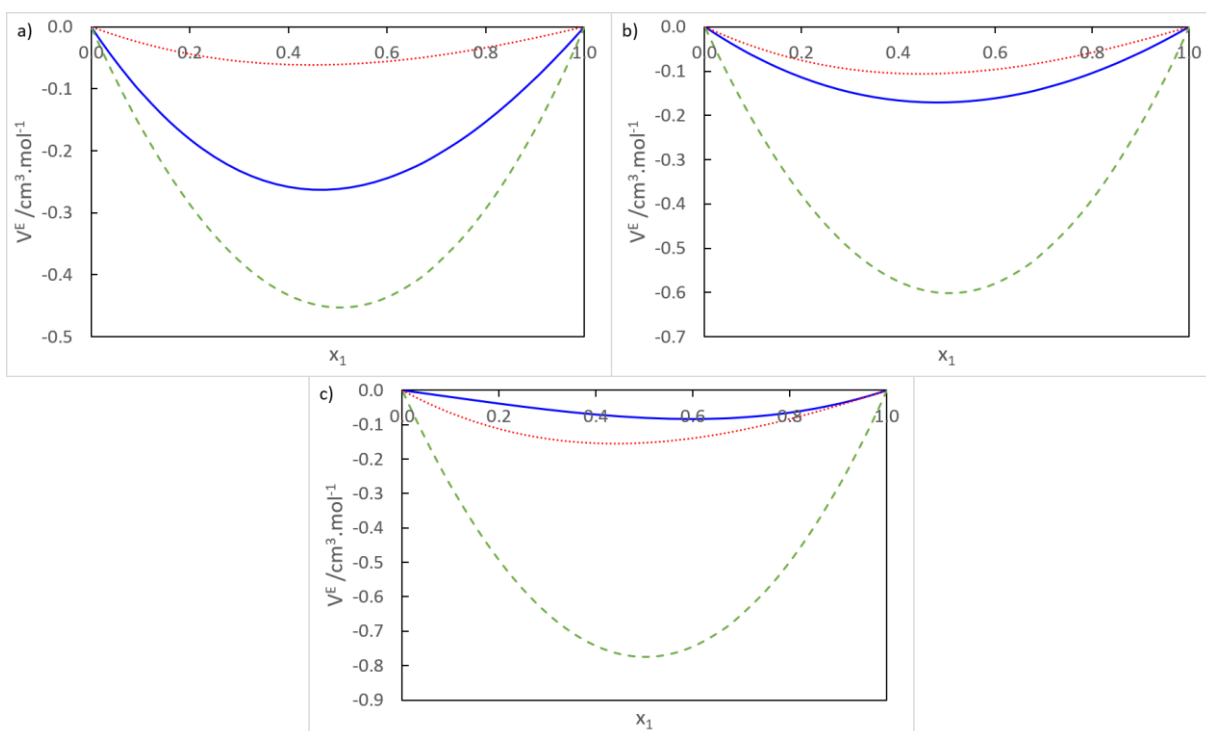


Figure 15: PFP contributions to v^E for DCE (1) + DIPE (2) system according to x_1 ; —: v_{int} , ...: v_{fv} , --: v_{P^*} ; a) $T = 283$ K, b) $T = 308$ K and c) $T = 333$ K.

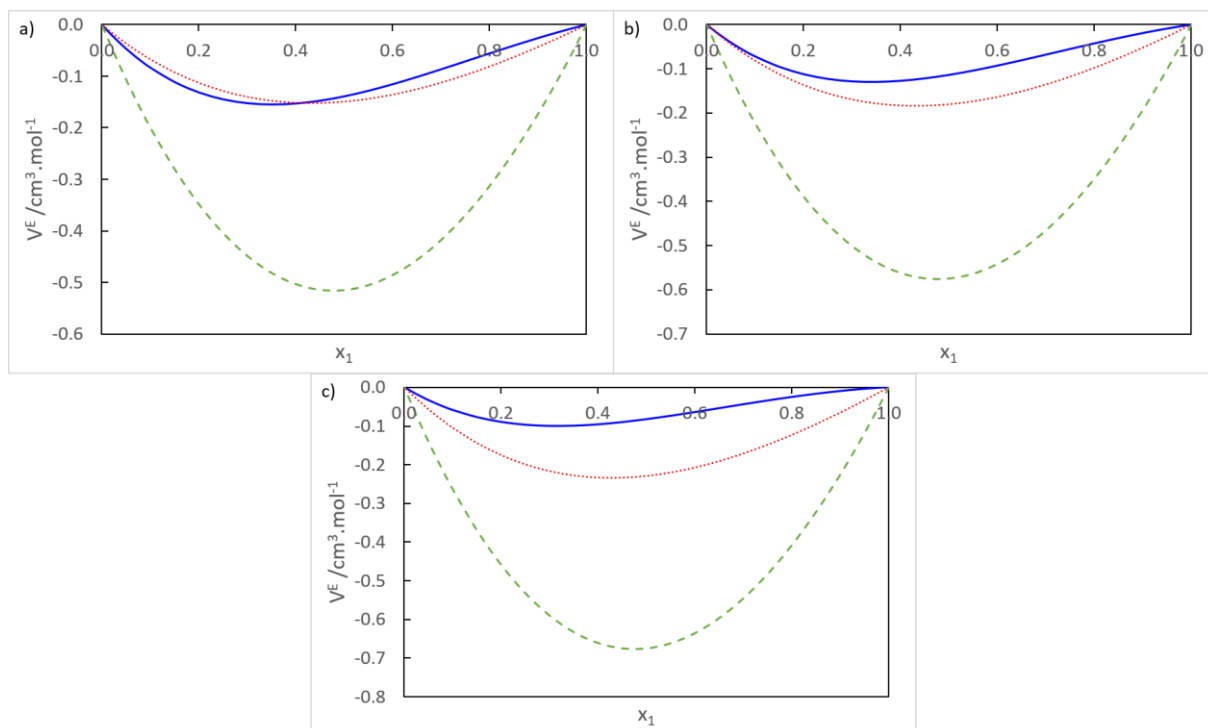


Figure 16: PFP contributions to v^E for DCE (1) + DEE (2) system according to x_1 ; —: v_{int} , ...: v_{fv} , -.-: v_{P^*} ; a) $T = 283$ K, b) $T = 293$ K and c) $T = 308$ K.

6. Conclusion

The densities of the DCE + MTBE, DCE + DIPE, and DCE + DEE binary solutions were determined at atmospheric pressure and temperature $T = (278.15 \text{ to } 333.15)$ K. The pure compound densities and speed of sound were also measured with a vibrating tube density meter. Furthermore, the excess molar volumes of these mixtures were estimated and correlated using the Redlich-Kister correlation. The excess molar volumes of the three binary systems are negatives for all the systems and in all the temperature range. The excess molar volume increases when the temperature increases for all the binary mixtures. We notice that the maximal absolute v^E for the three systems increases following: DCE + MTBE < DCE + DIPE < DCE + DEE. Accordingly, this amplitude difference between the three systems is due to the steric hindrance of the different ethers. The partial volume data treatment was also applied. The PFP theory was used as well on the three systems using a χ_{12} parameter. When this Flory parameter is dependent on the composition of the solution, a better representation of the experimental results for the DCE + MTBE mixture is found. According to the PFP model, the most relevant contribution for all these mixtures is the internal pressure and reduced volume, P^* contribution.

Supporting Information Available:

Evaluation of pure component densities, comparison with DIPPR correlation²³ and literature data²⁴⁻⁴⁰

7. References

- (1) Mehlman, M. A. Ethers; American Cancer Society, 2012.
- (2) Chapter 11 - Process Design. In Lees' Loss Prevention in the Process Industries (Fourth Edition); Mannan, S., Ed.; Butterworth-Heinemann: Oxford, 2012; 443–508.

- (3) Valtz, A.; Coquelet, C.; Boukais-Belaribi, G.; Dahmani, A.; Belaribi, F. B. Volumetric Properties of Binary Mixtures of 1,2-Dichloroethane with Polyethers from (283.15 to 333.15) K and at Atmospheric Pressure. *J. Chem. Eng. Data* 2011, 56, 1629–1657.
- (4) Amireche-Ziar, F.; Richon, D.; Belaribi, F. B. Excess Molar Enthalpies for Binary Mixtures of 1,2-Dichloroethane with Ethers at 298.15K and Atmospheric Pressure. *Fluid Phase Equilibria* 2013, 337, 255–258.
- (5) Amireche-Ziar, F.; Boukais-Belaribi, G.; Jakob, A.; Mokbel, I.; Belaribi, F. B. Isothermal Vapour–Liquid Equilibria of Binary Systems of 1,2-Dichloroethane with Ethers. *Fluid Phase Equilibria* 2008, 268, 39–44.
- (6) Benabida, H.; Coquelet, C.; Belaribi, F. B. Densities and Excess Molar Volumes of the Ternary System (1,4-Dioxane + 2-Propanol + 1,1,2,2-Tetrachloroethane) at T = 288.15–318.15 K and at Atmospheric Pressure: Experimental Measurements and Prigogine–Flory–Patterson Modeling. *J. Chem. Eng. Data* 2019, 64, 5122–5131.
- (7) Redlich, O.; Kister, A. T. Algebraic Representation of Thermodynamic Properties and the Classification of Solutions. *Ind. Eng. Chem.* 1948, 40, 345–348.
- (8) Patterson, D.; Delmas, G. Corresponding States Theories and Liquid Models. *Discuss. Faraday Soc.* 1970, 49, 98.
- (9) Flory, P. J. Statistical Thermodynamics of Liquid Mixtures. *J. Am. Chem. Soc.* 1965, 87, 1833–1838.
- (10) Abe, A.; Flory, P. J. The Thermodynamic Properties of Mixtures of Small, Nonpolar Molecules. *J. Am. Chem. Soc.* 1965, 87, 1838–1846.
- (11) Prigogine, I. *Molecular Theory of Solutions*, North Holland Publishing.; North-Holland Pub. Co.; New York: Amsterdam, 1957.
- (12) Hansen, C. M. *Hansen Solubility Parameters: A User’s Handbook*, Second Edition, 2nd ed.; CRC Press: Boca Raton, 2007.
- (13) Afzal, W.; Valtz, A.; Coquelet, C.; Richon, D. Volumetric Properties of (Piperidine+water) Binary System: Measurements and Modeling. *J. Chem. Thermodyn.* 2008, 40, 47–53.
- (14) Coquelet, C.; Auger, E.; Valtz, A. Density and Excess Volume for Four Systems Involving Eugenol and Furan. *J. Solut. Chem.* 2019, 48, 455–488.
- (15) Chirico, R. D.; Frenkel, M.; Magee, J. W.; Diky, V.; Muzny, C. D.; Kazakov, A. F.; Kroenlein, K.; Abdulagatov, I.; Hardin, G. R.; Acree Jr, W. E. Improvement of Quality in Publication of Experimental Thermophysical Property Data: Challenges, Assessment Tools, Global Implementation, and Online Support. *J. Chem. Eng. Data* 2013, 58, 2699–2716.
- (16) Desnoyers, J. E.; Perron, G. Treatment of Excess Thermodynamic Quantities for Liquid Mixtures. *J. Solut. Chem.* 1997, 26, 749–755.
- (17) Sharma, S. C.; Joshi, I. M.; Singh, J.; Gupta, A. Excess Molar Volumes of Methyl Tert-Butyl Ether with Chloroalkanes at 30°C. *J. Solut. Chem.* 1992, 21, 8.
- (18) Góralski, P.; Tkaczyk, M.; Chorążewski, M. Heat Capacities of α,ω -Dichloroalkanes at Temperatures from 284.15 K to 353.15 K and a Group Additivity Analysis. *J. Chem. Eng. Data* 2003, 48, 492–496.
- (19) Lemmon, E. W.; Huber, M. L.; McLinden, M. O. NIST Standard Reference Database 23: Reference Fluid Thermodynamic and Transport Properties-REFPROP, Version 8.0. 2007.
- (20) Páramo, R.; Zouine, M.; Sobrón, F.; Casanova, C. Oxygenated Gasoline Additives: Saturated Heat Capacities between (277 and 355) K. *J. Chem. Eng. Data* 2004, 49, 58–61.
- (21) Counsell, F.; A. Lee, D.; Martin, F. J. Thermodynamic Properties of Organic Oxygen Compounds. Part XXVI. Diethyl Ether. *J. Chem. Soc. Inorg. Phys. Theor.* 1971, 0, 313–316.
- (22) Ali Raza, M.; Valtz, A.; Coquelet, C.; Hallett, P. D.; Afzal, W. Volumetric Properties of Furan and 2-5-Dimethylfuran in Different Industrial Solvents at Temperatures from 278 to 343 K. *J. Chem. Eng. Data* 2021, 66, 2666–2680.
- (23) R.L. Rowley, W.V. Wilding, J.L. Oscarson, Y. Yang, N.A. Zundel, T.E. Daubert, R.P. Danner DIPPR Data Compilation of Pure Chemical Properties Design Institute for Physical Properties. 2006 Provo, UT: Brigham Young University.
- (24) Chorazewski, M.; Postnikov, E. B.; Oster, K.; Polishuk, I. Thermodynamic properties of 1, 2-dichloroethane and 1, 2-dibromoethane under elevated pressures: experimental results and

- predictions of a novel DIPPR-based version of FT-EoS, PC-SAFT, and CP-PC-SAFT *Ind. Eng. Chem. Res.*, 2015, 54, 9645-9656
- (25) Comelli, F. Excess enthalpies of 1, 3-dioxolane with 1, 2-dichloroethane and 1-bromo-2-chloroethane *Chim. Ind. (Milan, Italy)*, 1990, 72, 135-8
 - (26) Tafat-Igoudjilene, O.; Daoudi, H.; Hassein Bey-Larouci, A.; Aitkaci, A. Volumetric properties of binary liquid mixtures of ketones with chloroalkanes at different temperatures and atmospheric pressure *Thermochim. Acta*, 2013, 561, 63-71
 - (27) Klofutar, C.; Paljk, S.; Golc-Teger, S. Partial molar volumes and partial molar expansibilities of cholesterol in some aprotic solvents *Thermochim. Acta*, 1992, 196, 401-413
 - (28) Manfredini, M.; Marchetti, A.; Sighinolfi, S.; Tassi, L.; Ulrici, A. ; Vignali, M. Densities and excess molar volumes of binary mixtures containing 1, 2-dichloroethane+ 2-methoxyethanol or 1, 2-dimethoxyethane at different temperatures *J. Mol. Liq.*, 2002, 100, 163-181
 - (29) Garriga, R.; Andres, Ana Cristina; Perez, P.; Gracia, M. Vapor pressures at several temperatures and excess functions at 298.15 K of butanone with di-n-propyl ether or diisopropyl ether *J. Chem. Eng. Data*, 1999, 44, 296-302
 - (30) Gonzalez-Olmos, R.; Iglesias, M.; Santos, B. M. R. P.; Matted, S. Thermodynamics of oxygenate fuel additives as a function of temperature *Phys. Chem. Liq.*, 2008, 46, 223-237
 - (31) Meng, X.; Wu, J.; Liu, Z. Viscosity and density measurements of diisopropyl ether and dibutyl ether at different temperatures and pressures *J. Chem. Eng. Data*, 2009, 54, 2353-2358
 - (32) Montano, D. F.; Martin, S.; Cea, P.; Lopez, M. C.; Artigas, H. Volumetric, acoustic, and refractive properties of isomeric chlorobutanes with diisopropyl ether *J. Chem. Eng. Data*, 2010, 55(12), 5953-5959
 - (33) Pandiyan, V.; Oswal, S. L.; Vasantharani, P. Thermodynamic and acoustic properties of binary mixtures of ethers. III. Diisopropyl ether or oxolane with o-or m-toluidines at 303.15, 313.15 and 323.15 K *Thermochim. Acta*, 2011, 516, 64-73
 - (34) Evans, T.W.; Edlund ; K.R. Evans, T. W.; Edlund, K. R. (1936). Tertiary Alkyl Ethers Preparation and Properties *Ind.Eng.Chem.*, 1936, 28, 1186-1188
 - (35) Landaverde-Cortes, D.C.; Estrada-Baltazar, A.; Iglesias-Silva, G.A.; Hall, K.R. Densities and Viscosities of MTBE+ Heptane or Octane at p= 0.1 MPa from (273.15 to 363.15) K *J.Chem.Eng.Data*, 2007, 52, 1226-1232
 - (36) Meng, X.; Zheng, P.; Wu, J.; Liu, Z. Density and viscosity measurements of diethyl ether from 243 to 373 K and up to 20 MPa *Fluid Phase Equilib.*, 2008, 271, 1-5
 - (37) Oudemans, A.C. Sur la densité, le coefficient de dilatation et l'indice de réfraction de l'éther éthylique *Recl. Trav. Chim. Pays-Bas*, 1885, 4, 269
 - (38) Taylor, R. S.; Smith; L. B. Taylor; R. S. ;Smith, L. B. The vapor pressures, densities and some derived quantities for ether at low temperatures *J. Am. Chem. Soc.* 1922, 44, 2450-2463
 - (39) Timmermans, J. Measurements of the Density of Liquids at Temperatures Below 0 *Sci. Proc. R. Dublin Soc.* 1912, 13, 310
 - (40) Young, S. The vapour-pressures, specific volumes, heats of vaporization, and critical constants of thirty pure substances *Sci. Proc. R. Dublin Soc.* 1910, 12, 374-443.

TOC Graphic

